




# Parametric Optimization of a New Gear Pump Casing Based on Weight Using a Finite Element Method

Olga Zharkevich <sup>1</sup>, Tatyana Nikonova <sup>1</sup>, Łukasz Gierz <sup>2,\*</sup>, Andrey Berg <sup>1</sup>, Alexandra Berg <sup>1</sup>, Darkhan Zhunuspekov <sup>1</sup>, Łukasz Warguła <sup>2</sup>, Wikotor Łykowski <sup>2</sup> and Ksawery Fryczyński <sup>2</sup>

<sup>1</sup> Department of Technological Equipment, Mechanical Engineering and Standardization, Abylka Saginov Karaganda Technical University, Karaganda 100027, Kazakhstan; zharkevich82@mail.ru (O.Z.); nitka82@list.ru (T.N.); 22526633@mail.ru (A.B.); kibeko\_1995@mail.ru (A.B.); zhynyspekov\_darkhan@mail.ru (D.Z.)

<sup>2</sup> Institute of Machine Design, Faculty of Mechanical Engineering, Poznan University of Technology, 60-965 Poznan, Poland; lukasz.wargula@put.poznan.pl (Ł.W.); wiktor\_lykowski@o2.pl (W.Ł.); ksawery.fryczyński.pp@gmail.com (K.F.)

\* Correspondence: lukasz.gierz@put.poznan.pl; Tel.: +48-782-169-798

**Abstract:** Reducing the weight of the structures and choosing the materials used in mechanical engineering is an important and pressing economic and environmental problem. The design of a gear pump is developed from the point of view of the geometry of the gears, as well as the casing. This paper tested a gear pump casing using the environment of the ABAQUS 2020 system in the field of statistical strength analysis using the finite element method. The tests were carried out on the pump body and the front and rear covers, which were made of three types of materials (cast iron, aluminum, and polycarbonate), at a pressure of 28 MPa. After loading, the maximum stresses in the aluminum casing (177 MPa), the cast iron casing (157 MPa), and the polycarbonate (200 MPa) were determined. The largest stress concentrators are the grooves at the bottom of the pump casing. Rounding the internal chamber of the casing with a radius of 4 mm made it possible to reduce stress in this zone by 10 MPa. The parametric optimization of the front and back covers of the gear pump made it possible to reduce the total weight of the aluminum structure by 14%, the cast iron by 12%, and the polycarbonate by 16%. The 3D models show areas of minimal stress where the size and weight of the structure could be reduced in the future using a comprehensive approach involving parametric and topological analysis.

**Keywords:** simulation; part; stress; safety factor; fatigue



**Citation:** Zharkevich, O.; Nikonova, T.; Gierz, Ł.; Berg, A.; Berg, A.; Zhunuspekov, D.; Warguła, Ł.; Łykowski, W.; Fryczyński, K. Parametric Optimization of a New Gear Pump Casing Based on Weight Using a Finite Element Method. *Appl. Sci.* **2023**, *13*, 12154. <https://doi.org/10.3390/app132212154>

Academic Editor: Nikolaos Koukoulas

Received: 26 September 2023

Revised: 6 November 2023

Accepted: 6 November 2023

Published: 8 November 2023



**Copyright:** © 2023 by the authors. Licensee MDPI, Basel, Switzerland. This article is an open access article distributed under the terms and conditions of the Creative Commons Attribution (CC BY) license (<https://creativecommons.org/licenses/by/4.0/>).

## 1. Introduction

This article is a study of the design of a five-gear pump and includes the modeling of its strength in ABAQUS 2020, the subsequent development of recommendations for the optimization of the geometric dimensions, the casing, and the front and rear covers, and the choice of material to reduce the weight of the entire pump structure.

Gear pumps are widely used in many industries due to their reliability, simplicity of design, compactness, and efficiency [1,2]. Gear pumps are positive displacement type pumps. Gear pumps are generally used to pump liquids with high viscosity: fuel oils, oils, lubricating oils, paints, acids and alkalis, alcohols, and solvents [3–5]. In a gear pump, the rotation of the pump is transmitted by the drive gear [6]. The drive gear rotates through contact with the drive gear. The liquid is transported from the suction side to the discharge side of the pump (from the input port to the outlet port) [7]. A gear pump moves fluid by repeatedly enclosing a fixed volume within interlocking gears, mechanically transferring it to provide a smooth, impulse-free flow proportional to the speed of rotation of its gears [8]. In this case, a tight contact is formed between the teeth, as a result of which the reverse transfer of liquid from the discharge cavity to the suction cavity is impossible [9].

There are several types of external gear pump designs. These designs differ due to the presence of two, three, or four driven gears located on one axis (Figure 1) and the presence of three or four driven gears located around the drive gear (Figure 2).

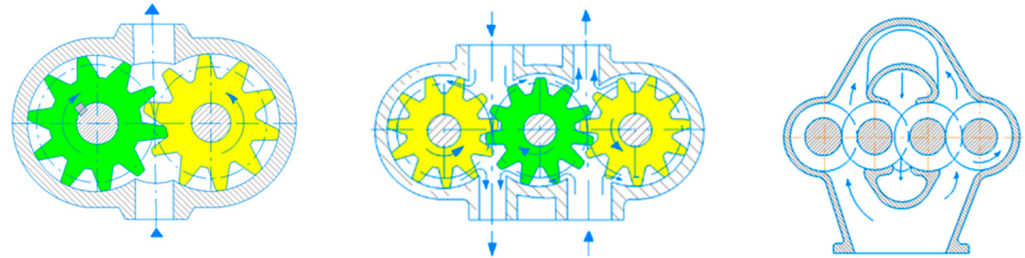


**Figure 1.** Designs of external gear pumps with different numbers of driven gears on the same axis [10–13].

External gear pumps with three gears are advantageous for use in hydraulic drives in which it is necessary to have two hydraulic lines with independent pressure [14].

The design of an external gear pump with four gears on one axis increases the pump energy intensity [15].

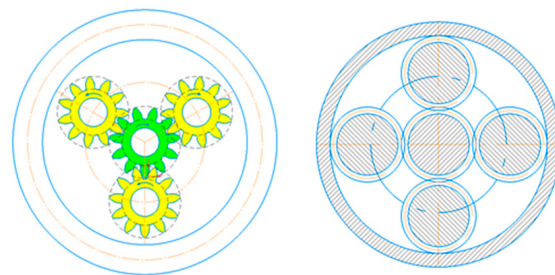


**Figure 2.** Designs of external gear pumps with driven gears around the drive axis [16,17].

Depending on the location of the gears, the shape of the casing is selected when designing a gear pump and the material from which it will be made.

To facilitate the design of the gear pumps, the casings are usually made of aluminum [18]. Gray cast iron is also used for gear casings [19]. Reducing the weight of a gear pump greatly affects the geometry of the structure [20]. However, if the hull geometry is reduced too much, it will reduce the structural strength below the limiting value. Therefore, it is necessary to determine the optimal geometry of the gear pump casing with small dimensions and the appropriate strength criteria. In view of this, gear pump casings often have irrational designs in terms of material consumption [21]. When obtaining the geometric dimensions of the gear pump casing, the designers try to obtain a less labor-intensive method to manufacture the structure, even one which is universal with respect to the operating modes of the pumps [22].

Also important in the design of gear pumps is the identification of dangerous sections of the structure in areas of stress concentration [23].

The key design stage in the determination of the optimal dimensions of the casing is the calculation of static strength [24]. This calculation is limited to the use of empirical dependencies and is labor-intensive [25]. The complexity of the calculations is explained by the large volume of analytical loads that act on the body. Furthermore, the difficulty of the calculations is due to the fact that the analytical methods for determining the stress–strain state of a structure are limited to simple load diagrams and primitive geometry [26].

For newly created structures, it is difficult to immediately select the optimal dimensions; therefore, after obtaining a calculation model and identifying its shortcomings or potential capabilities, the designers resort to optimization. It is important that the solutions obtained during the optimization process are both technologically advanced and functional [27]. Design optimization does not mean an abstract search for the most ideal shape, but rather the application of mathematical methods to find a solution that meets a certain quality criterion (or optimality indicator) and the specified constraints in the geometric shape and dimensions of a given structure [28].

There are several parametric optimization methods (Table 1).

**Table 1.** The parametric optimization method.

Method	Object	Result	Reference
Fuzzy logic and ANFIS	gripper mechanism	geometry parameters	[29]
Function deployment	rotary pump	assembly of rotary pump with positive displacement	[30]
Artificial intelligence algorithm	centrifugal pump	area of cross-section volute casing, impeller side wall gap, volute casing tongue	[31]
FEM + Taguchi method	gear casing	topology and shape optimization of gear casing	[32]
CFD + FEM	boiler circulating pump's casing	structural tightness of the casing	[33]
NSGA-II	centrifugal pump	structural parameters	[34]

For more efficient body parts, computational and graphical methods with an additive quality criterion [35] and methods of differential and integral calculus with a multiplicative quality criterion [36] are also used.

In this article, to optimize the casing design of a gear pump, it is recommended to use a penalty function model, which is built on the basis of restrictions  $g$  on the quality of the casing design (safety factor), and the target function  $F$  is the reduced mass. This model is based on the Davidon–Fletcher–Powell method [37].

The quality of the design solutions is assessed based on the presence of such criteria as efficiency  $F$  (casing weight) and quality  $g$  (quality criterion). When the required result is achieved, the efficiency criterion must be minimized, and the quality criterion must tend to certain specified values of  $g$ .

This article is a study of the design of a new five-gear pump; the study includes the modeling of its strength in ABAQUS and the subsequent development of recommendations for the optimization of the geometric dimensions, the casing, and the front and back covers, as well as the choice of material to reduce the weight of the entire pump structure. The strength analysis of the gear pump casing design shows areas where efforts can be made to reduce weight.

## 2. Materials and Methods

### 2.1. Object of Study

The purpose of the study is a new design of a gear pump with 5 gears (Figure 3). The purpose of creating a new gear pump with 5 gears is to increase efficiency when pumping liquids of various natures, to increase its reliability, to reduce its size, and to reduce the cost of the entire structure.

The back cover is screwed to the body with 8 bolts. The operating diagram of the gear pump with 5 gears is shown in Figure 4.

The liquid is pumped along the red line, and suction is carried out along the green line. The liquid enters or is sucked out through four openings in the casing (visible from the outside). The inlet pipes of an oil tank are attached to these injection ports.

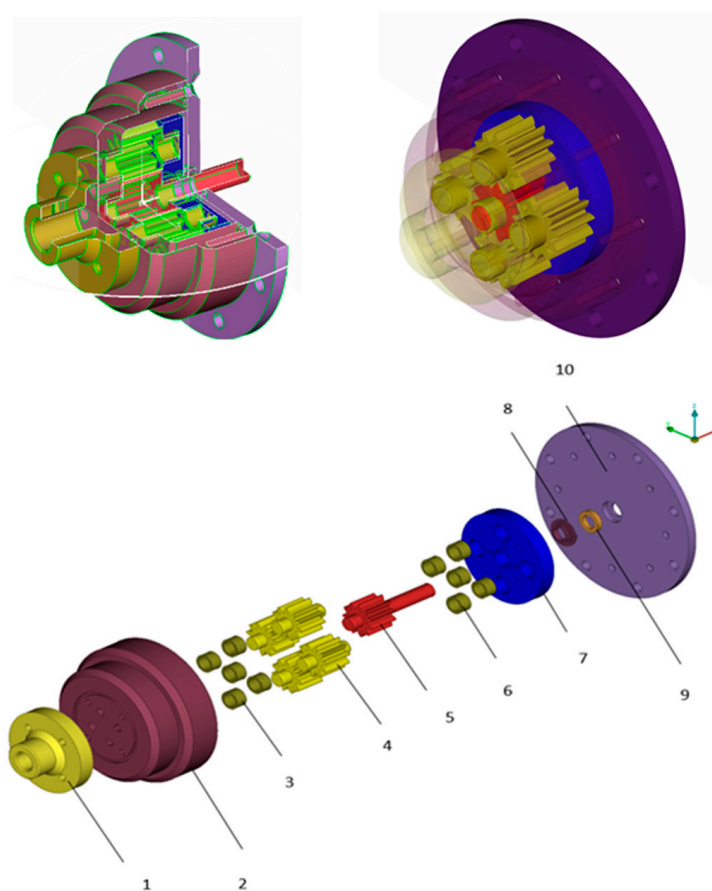


**Figure 3.** Design of a gear pump with 5 assembled gears: 1—front cover; 2—casing; 3, 6—bearings; 4—driven gears; 5—drive gear on the drive shaft; 7—flange; 8—seal; 9—retainer ring; 10—back cover.

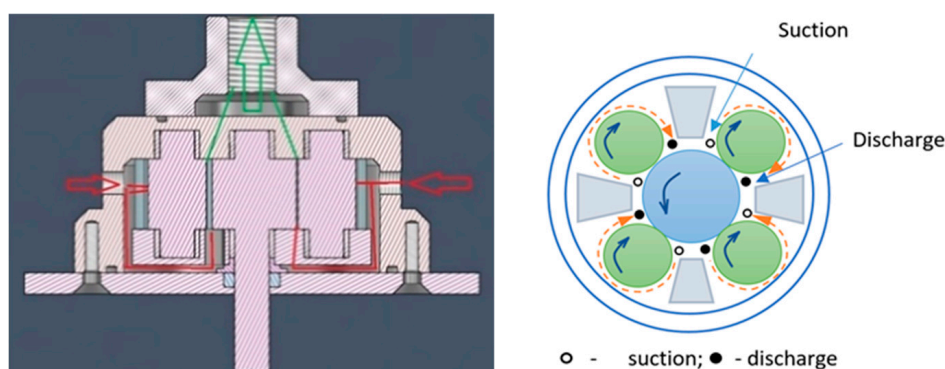


**Figure 4.** Diagram of fluid flow in the gear pump with 5 gears.

## 2.2. Creating a Model of the Research Object

The casing calculation was performed by FEM in ABAQUS.

The choice of material for the casing of a new gear pump (Table 2) should be justified by strength calculations. The most common materials for such pumps were chosen for the pump casing of the new design: aluminum (Europe), cast iron (Kazakhstan), and a composite material, polycarbonate (China).



**Table 2.** Material properties.

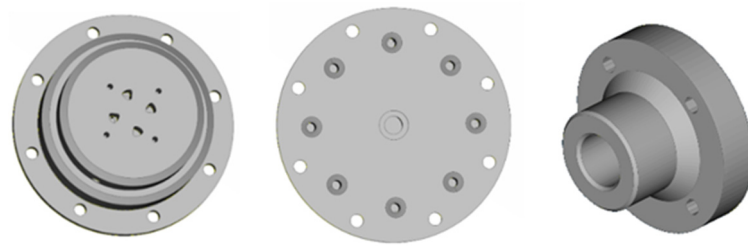
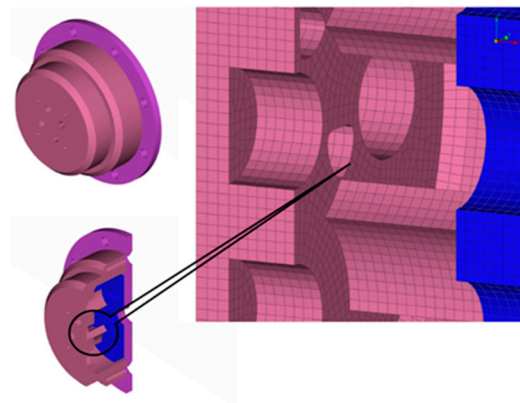
Material	Yield Strength, MPa	Tensile Strength, MPa	Tensile Modulus, GPa	Poisson's Ratio	Density, kg/m <sup>3</sup>
Aluminum (PA6 alloy)	250	390	72.5	0.33	2790
Cast iron (QT450-10)	310	450	120	0.257	7060
Polycarbonate	280	300	16.5	0.46	2074

These materials have the isotropic behavior of the material, which is characterized by the Young modulus and the Poisson ratio [38].

This study applies the von Mises yield criterion and the Prandtl–Reuss flow rule to create a stress–strain equation for an elasto-plastic material with isotropic properties [39].

The simulation was carried out for three parts of the pump: the casing, the back, and the front cover. The dimensions of the new gear pump parts were calculated analytically using machine theory.

To model each part, a solid model was made, which was then divided into elements. Figure 5 shows an example of a solid model of a gear pump casing with back and front covers. Figure 6 shows an example of a finite element model of a hull.

**Figure 5.** Solid model of the casing with front and back covers.**Figure 6.** Finite element model of the hull.

When creating a computational model for analysis, a standard procedure is performed to apply a finite element mesh. In the meshing process, three-dimensional second-order HEXA FEMs (hexa elements) were used. HEXA FEM (hexa elements) is the best element for modeling; in turn, when modeling, the use of TETRA FEM is avoided, since this type of element concentrates stress in the structure of the model. To accurately represent the distribution of internal stresses in samples under the influence of external forces, it is necessary to pay due attention to the distribution of the finite element mesh. The validity of the results depends on the quality of the network. To achieve optimal mesh quality, quality criteria for a finite element mesh were used (Figure 7). The number of elements that do not pass the quality criteria is less than 1% of the total number of elements (Figure 8), which is

the optimal value. The total number of elements of the model is 163,292, of which 12 are tetras; this is less than 1% and is acceptable for this model (Figure 8).

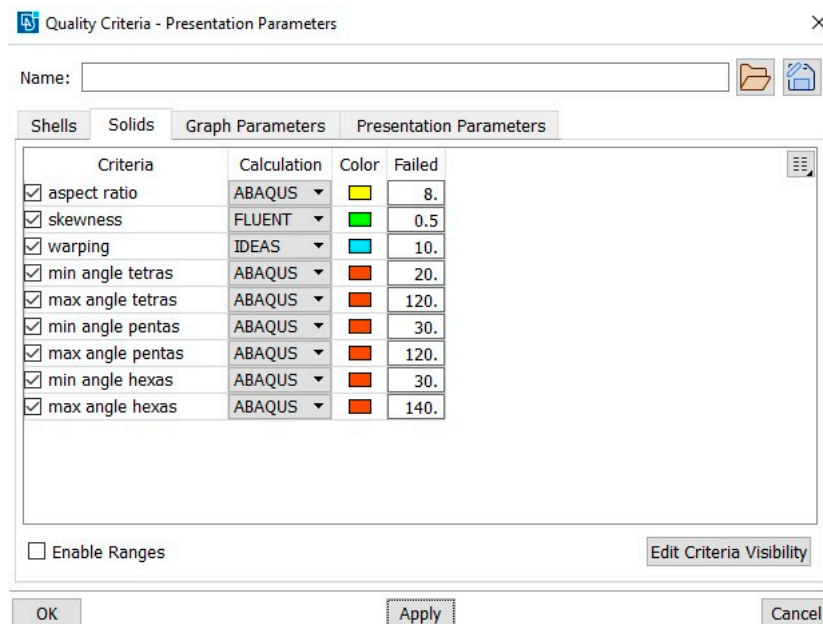


**Figure 7.** Quality criteria for a volumetric finite element network.

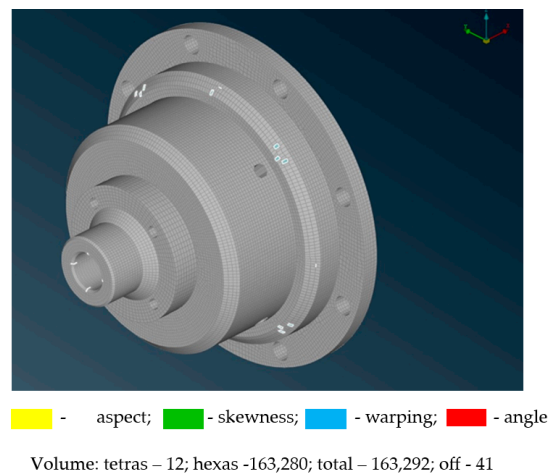


**Figure 8.** Total number of elements that do not match.

### 2.3. Applying Loads and Setting Boundary Conditions

The following loads were assumed for the simulation:

- Loads on the surfaces of the casing, loads on the rear cover for shaft mounting, loads on the front cover along the fluid outlet channel;
- Loads on the cylindrical surfaces of the casing sealed along the periphery of the gear zone.

These loads were determined analytically.

The maximum pressure was 28 MPa.

The amount of radial load applied to each shaft seating surface corresponds to the reaction force acting on the pump supports during operation.

The calculation was performed using dependencies that assume the nonlinear and parabolic nature of the law of pressure distribution in the gap between the gears [40]. The

resulting force is determined by the sum of the forces caused by the hydraulic load in the peripheral gap, the pressure in the discharge zone, and the force from the transmitted torque.

To obtain a correct solution to the problem, the appropriate restrictions were set for the model (Figure 9):

- Fixation under all bolt holes in the rear cover of the pump (zero movements along all axes X, Y, Z;

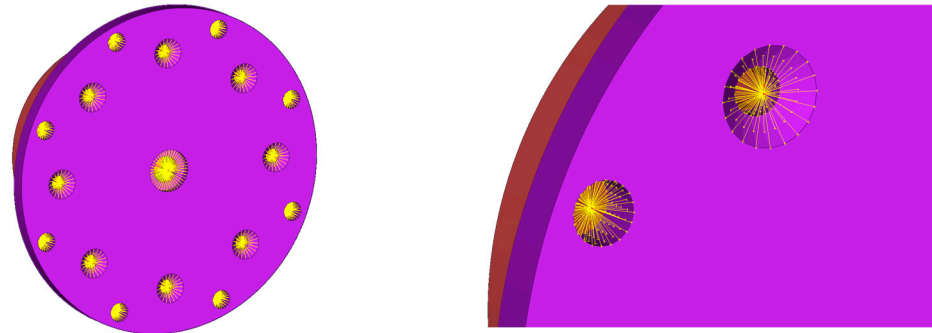


Figure 9. Model boundary conditions.

Fixation of vertical movements of the lower surface of the case, which is attached to the back cover (zero movements along the Y axis).

The fixations are represented by yellow lines connecting the slave nodes to the master node, which is drawn as a red cross.

#### 2.4. Determination of the Safety Factor $n$ and Fatigue Strength of the Structure

A strength coefficient was used to assess the structural strength of the gear pump parts. The strength coefficient is determined by the formula [41]:

$$n = \frac{\sigma_s}{\sigma_{max}} \quad (1)$$

where  $\sigma_s$ —tensile strength of the material, MPa;  $\sigma_{max}$ —maximum stress in the structure, MPa.

To analyze the fatigue strength and the nature of the stress propagation in the gear pump, the calculation method presented in the FKM manual [42] was used. According to this technique, the readings of the characteristics of the internal stress are taken from two points, taking into account the distance between them and calculating the stress gradient (Figure 10).

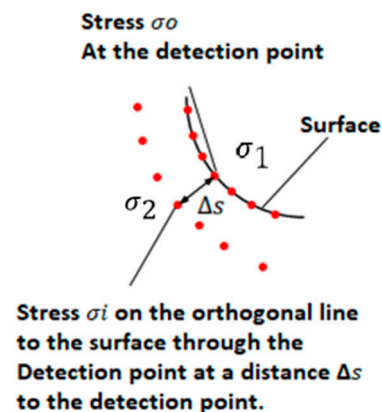


Figure 10. Stress amplitudes determined by points [42].

The initial loading condition for the model is the average value of the loading cycles of at least  $1 \times 10^7$ .

### 2.5. Determination of the Dependence of Stresses on the Geometric Parameters of the Structure

This section may be divided into subheadings. It should provide a concise and precise description of the experimental results, their interpretation, and the experimental conclusions that can be drawn.

To check the dependence of stress on the geometric parameters of the structure, regression analysis will be used with the compilation of a quadratic regression Equation (2) and the subsequent proof of its suitability [43].

$$Y = ax^2 + bx + c \quad (2)$$

where  $a, b, c$ —regression coefficients;  $x$ —variable value.

The coefficients  $a, b$ , and  $c$  are defined by the matrix [43]:

$$\begin{cases} a \sum x_i^2 + b \sum x_i + nc = \sum y_i \\ a \sum x_i^3 + b \sum x_i^2 + c \sum x_i = \sum x_i y_i \\ a \sum x_i^4 + b \sum x_i^3 + c \sum x_i^2 = \sum x_i^2 y_i \end{cases} \quad (3)$$

The correlation coefficient [44]:

$$R = \sqrt{1 - \frac{\sum (y_i - \hat{y}_i)^2}{\sum (y_i - \bar{y})^2}} \quad (4)$$

where  $\bar{y} = \frac{1}{n} \sum y_i$ .

The determination coefficient [44]:

$$D = R^2 \quad (5)$$

The average approximation error [44]:

$$\bar{A} = \frac{1}{n} \sum \left| \frac{y_i - \hat{y}_i}{y_i} \right| \cdot 100\% \quad (6)$$

Regression analysis calculates the estimated relationship between the dependent variable (stress) and the independent variable (geometric parameter).

### 2.6. Determination of the Design Optimization Criterion

The design optimization criterion using the Davidon–Fletcher–Powell method is determined by the formula [37]:

$$F = \frac{m}{m_0} + V \sum_{i=1}^n \frac{1}{\psi_i}, \quad (7)$$

where  $\psi_i = \frac{1}{1-g_i}$  — penalty functions;

$g_i$ —restrictions;

$V$ —volume;

$m_0$ —initial mass;

$m$ —final mass.

The optimality of the design solutions is determined by criteria such as efficiency  $F$  (casing weight) and quality  $g$  (quality criterion). When the required result is achieved, the efficiency criterion must be minimized, and the quality criterion must tend to certain specified values of  $g$ .

The pump design will be considered optimal if  $F(\bar{x}) \rightarrow \min$ ;  $g(\bar{x}) = g_0$ .

Moreover  $F(\bar{x}), g(\bar{x})$  are the given functions of the design variables.

The restrictions are formed on the safety factor ( $n$ ).

To determine the optimization criterion  $F$ , the volume of all the parts is constant ( $V = 1$ ).

### 3. Results

As a result of the simulation, the stress distributions in the gear pump casing were obtained (Figures 11 and 12). From the figures, it is clear that the most loaded part of the gear pump casing is the bottom of the casing along the entire diameter at the transition to the vertical surface of the wall. The maximum stresses in the aluminum casing are  $172 \div 177$  MPa (Figure 11). The maximum stresses in the cast iron casing are  $147 \div 157$  MPa (Figure 12). The maximum stresses in the polycarbonate casing are  $187 \div 200$  MPa (Figure 13).

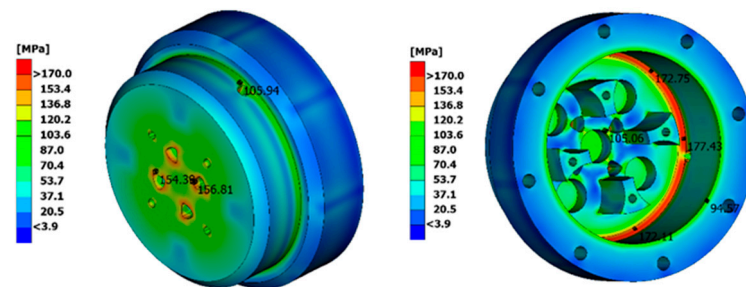


Figure 11. Stress value in the aluminum gear pump casing.

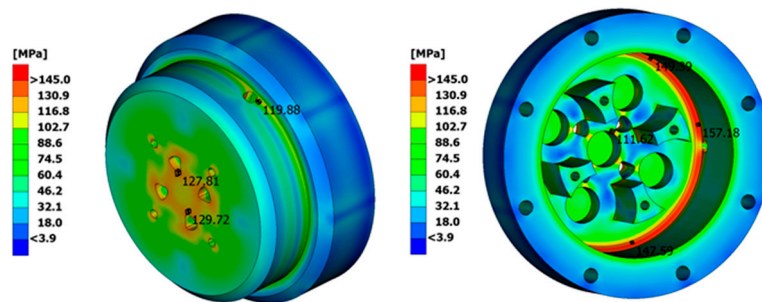


Figure 12. Stress value in a cast iron gear pump casing.

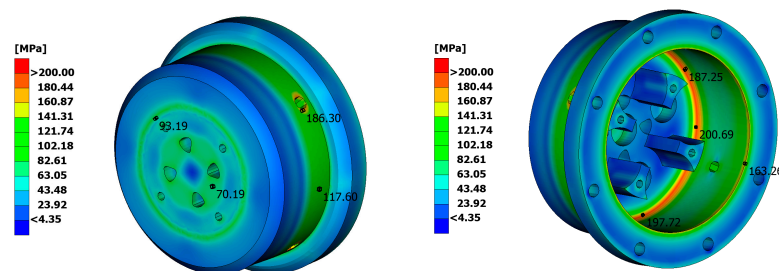


Figure 13. Stress value in a polycarbonate gear pump casing.

It is noted that the stress concentrators are the grooves in the grooves at the bottom of the pump casing.

The stresses in the pump back cover were also considered, since the operation of the bearings seated in the flange seats, when taking the radial load into account, affects the back cover of the casing (Figures 14–16).



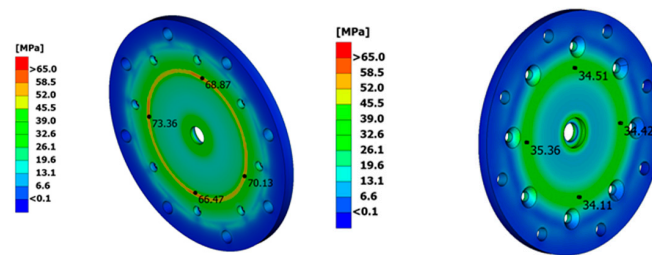


Figure 14. Stress value in the aluminum back cover of a gear pump.

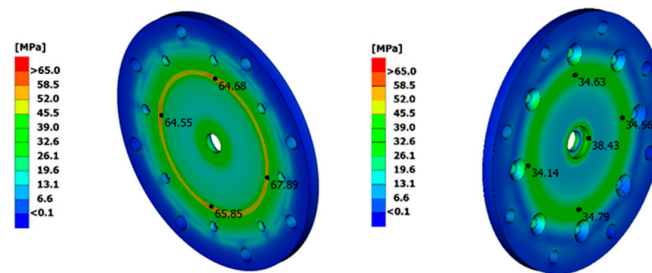


Figure 15. Stress value in the cast iron back cover of a gear pump.

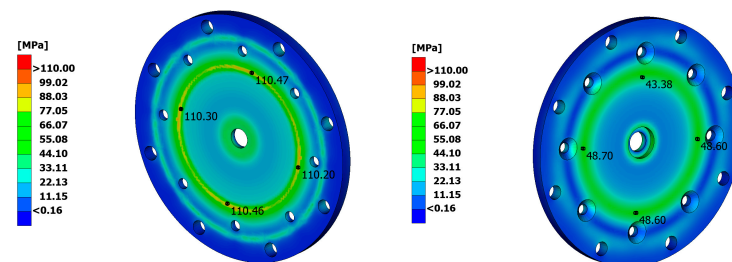


Figure 16. Stress value in the polycarbonate back cover of a gear pump.

The maximum stresses on the back cover of the aluminum, cast iron, and polycarbonate are shown in Table 3.

Table 3. Stresses in the back cover of the gear pump.

Aluminum	Cast Iron	Polycarbonate
35 ÷ 77 MPa	34 ÷ 67 MPa	43 ÷ 110 MPa

The most stressed part of the back cover of the gear pump casing is the middle part, which describes the contour on which the flange is located.

The visualization of the distributions in the front cover of the pump is presented in Figure 17.

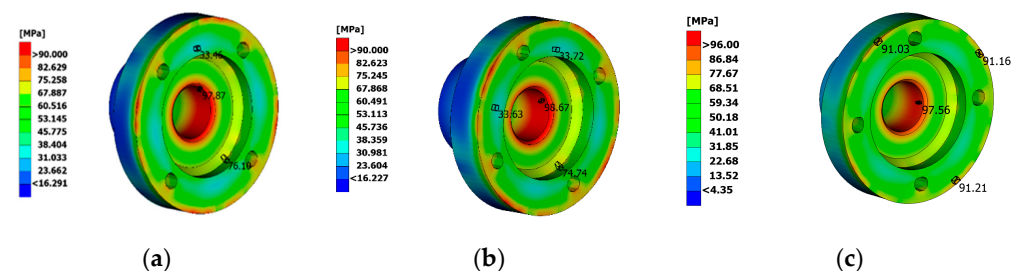


Figure 17. Stress value on the front cover of gear pump: (a) aluminum front cover; (b) cast iron front cover; (c) polycarbonate front cover.

Maximum stresses (97.87–98.67 MPa) are observed at the beginning of the liquid outlet channel in the front cover made of the three materials. This occurs due to the influence of centrifugal force.

#### 4. Discussion

##### 4.1. Assessment of the Safety Factor and Fatigue Strength of the Structure

Strength factors were determined to evaluate the strength of the casing and the front and back covers of the gear pump.

The calculated safety factors for the pump elements made of the various materials are given in Table 4.

**Table 4.** Calculated safety factors for casing, front cover, and back cover.

	Aluminum	Cast Iron	Polycarbonate
Casing	2.2	2.8	1.5
Back cover	5	6.7	2.7
Front cover	4	4.6	3.1

The standard safety factor of the parts in mechanical engineering is  $n \geq (1.5 \div 2.5)$  [45,46]. In 2017, Mancini et al., during a project in which they replaced metal parts with polymer composite materials in motorcycle oil pumps, assumed a safety factor of at least 1.6 [47]. In 2015, Kollek and Radziwonowska assumed a value of the safety factor of at least 2.9 for the body of a gear micropump [48].

From Table 2, it can be seen that the safety factor is maintained for all the parts of the pump structure made of aluminum, cast iron, and polycarbonate. In this case, the safety factor is higher than the standard for a cast iron body by 14.4–32%. The safety factor of the aluminum body complies with the standard. For the back and front covers, the safety factor exceeds the standard by 1.6–2 times. The safety factor of the polycarbonate body meets the standard. For the back and front covers, the safety factor exceeds the standard of 8–24%. This indicates that these structural parts of the gear pump are not overloaded.

The results of the fatigue strength calculations are presented in Table 5.

**Table 5.** Calculation results for the fatigue strength of the gear pump casing.

Material	Fatigue Strength, $\sigma_{BK}$ , MPa	Fatigue Strength Factor, $K_{BK}$
	Casing	
Aluminum	37.37	0.81
Cast iron	128.55	0.54
Polycarbonate (PC)	31.32	0.94
	Back cover	
Aluminum	17.54	0.38
Cast iron	58.76	0.21
Polycarbonate (PC)	10.4	0.70
	Front cover	
Aluminum	28.16	0.61
Cast iron	89.14	0.32
Polycarbonate (PC)	23.24	0.72

Based on the results of the fatigue strength assessment, it can be said that the gear pump parts considered have a level of redundancy in terms of damage resistance (Table 6). In 2022, Wang et al., during centrifugal pump studies, achieved improvements ranging from 38 to 62% [49].

**Table 6.** Level of resistance to damage to gear pump parts.

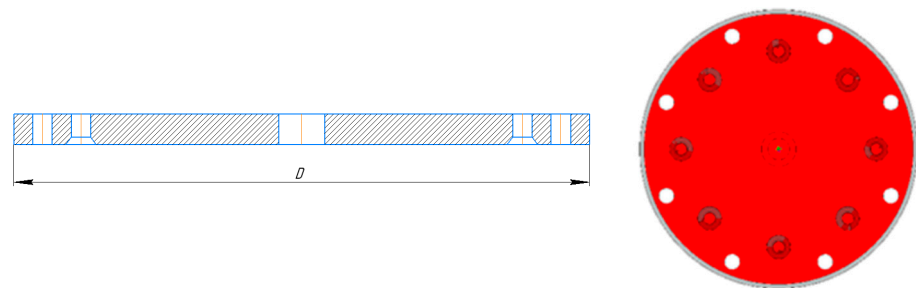
Material	Casing	Back Cover	Front Cover
Aluminum	19%	62%	38%
Cast iron	46%	81%	68%
Polycarbonate (PC)	6%	30%	28%

The results of the strength calculation of the parts of the new gear pump show that the pump design can be subjected to parametric optimization. Optimization should be carried out for the aluminum, cast iron, and polycarbonate casing because the safety factor is  $n \geq 1.5$ ).

#### 4.2. Optimization of Gear Pump Parts

##### 4.2.1. Optimization of Gear Pump Back Cover

As the pump back cover (Figure 18) has a large safety factor, but also a large number of mounting holes, optimization was carried out in terms of diameter.

**Figure 18.** Gear pump back cover.

Parametric optimization of the pump cover was carried out by diameter because the safety factor in this zone tends to infinity. Figure 18 shows in gray the zone that will be removed as a result of optimization.

By brute force, four variants of back covers were loaded (pressure 28 MPa), with an optimization step of 2 mm in the direction of the decrease. The results for the back cover are presented in Table 7.

**Table 7.** Optimization options for the pump back cover.

Variant	Diameter, D, mm	Maximum Stress, $\sigma_{max}$ , MPa	Weight, m, kg
Aluminum			
1 (original)	256	73.76	1.84
2	254	77.24	1.61
3	252	84.12	1.43
4	250	91.12	1.20
Cast iron			
1 (original)	256	67.89	6.90
2	254	73.24	6.51
3	252	79.01	6.14
4	250	85.16	5.52
Polycarbonate (PC)			
1 (original)	256	110.47	1.21
2	254	117.53	1.14
3	252	123.58	1.06
4	250	129.31	1.01

In all four variants (aluminum, cast iron, and polycarbonate), the standard safety factor is provided. The polycarbonate pump back cover has the minimal weight. The cast iron back cover has the maximal weight.

The subsequent reduction in the diameter of the cover is impossible because of the presence of the holes for fastening.

For the back cover of a pump made of three materials, the optimality criterion was calculated using Formula (1). The optimality criterion for the back pump cover is given in Table 8.

**Table 8.** The optimality criterion for the back pump cover.

Initial Mass, $m_0$ , kg	Final Mass, $m$ , kg	Safety Factor, $n$	Optimization Criteria, $F$
1.84	1.20	Aluminum	0.31
		Cast iron	
6.95	5.52	4.6	2.8
1.21	1.01	Polycarbonate (PC)	0.86
		2.7	

The polycarbonate back pump cover has a minimal weight. However, taking into account the mass ratios and safety factor, aluminum should be selected for the back pump cover. With this construction material, the optimization criterion is reduced to a minimum.

According to Formulas (2)–(6), a regression analysis was performed to establish a mathematical model of quadratic regression and its adequacy. The results show an inversely proportional relationship between the diameter of the cover ( $X$ ) and the maximum stresses ( $Y$ ). The dependence of the stress values on the diameter of the following cover has the form:

$$Y = 0.1750x^2 - 91.9290x + 12,132.9120$$

At the same time, the correlation coefficient is 0.99, the determination coefficient is 0.99, and the average approximation error is 0.23. The obtained correlation coefficient and determination coefficient show that the parameter relationship between the studied covers is very strong. As the approximation error is less than 15%, this equation can be used as a regression equation.

By changing the number and location of the holes in the back cover, the weight of this part can be further reduced. There is no analysis of the back and front covers in the literature; studies of casing [47,48,50–52] and pump impellers [53] predominate.

#### 4.2.2. Optimization of the Front Cover of the Gear Pump

To keep the diameter of the outlet unchanged, it was decided to optimize the design of the top cover (Figure 19) around the perimeter.

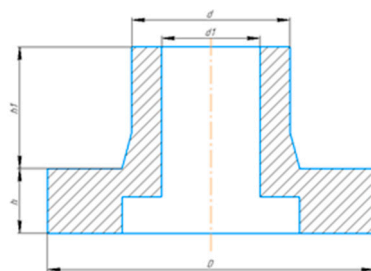


**Figure 19.** Gear pump front cover.

As there is the possibility of optimizing several parameters at once in the front cover of a gear pump, it was decided to select the optimal option based on an exhaustive search strategy. The variable geometric dimensions of the top cover are presented in Table 9. The

parameter  $d_1$  remains constant. During the simulation, the maximum stresses (Figure 20) and weights were determined.

**Table 9.** Front cover input and output parameters.

Design Variant	D, mm	d, MPa	h, mm	$h_1$ , mm	$\sigma_{\max 1}$ , MPa (Al)	$m_1$ , kg (Al)	$\sigma_{\max 2}$ , MPa (Cast Iron)	$m_2$ , kg (Cast Iron)	$\sigma_{\max 1}$ , MPa (PC)	$m_3$ , kg (PC)
1 variant	126	61	25	33	97.87	3.14	98.67	8.41	110.1	2.08
2 variant	124	60	24	32	103.5	2.78	100.4	7.81	113.4	1.99
3 variant	122	59	23	31	107.6	2.45	103.01	7.44	117.1	1.90
4 variant	120	58	23	30	110.3	2.18	106.01	7.07	120.3	1.80
5 variant	118	57	22	29	113.5	1.96	109.05	6.61	124.1	1.71
6 variant	116	56	22	28	117.5	1.59	112.3	6.18	127.2	1.59

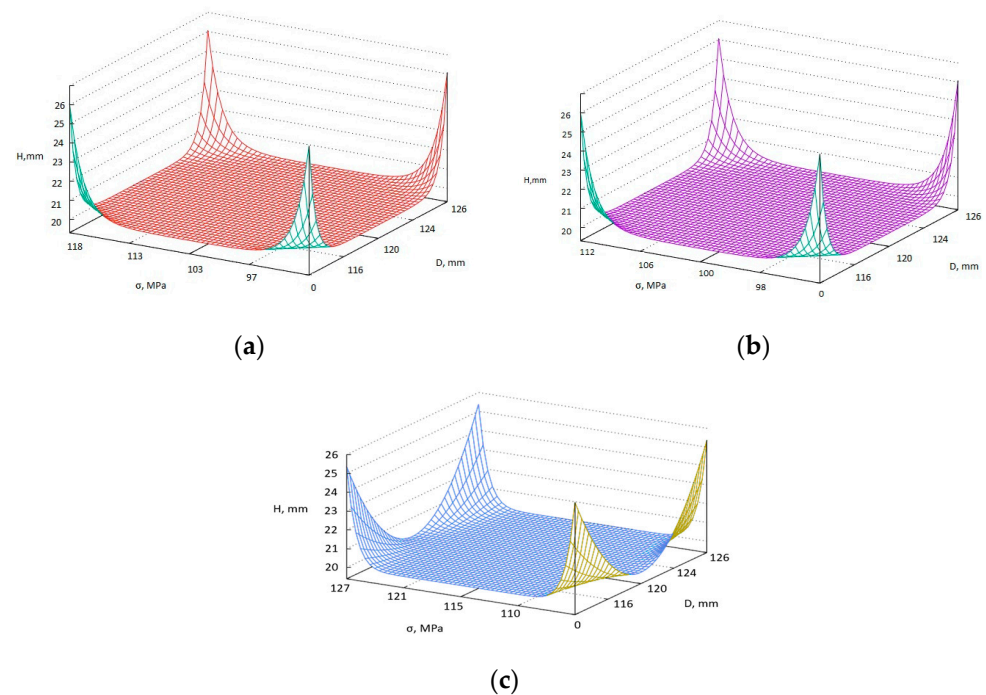


**Figure 20.** Stresses in various front cover designs: (a) aluminum front cover; (b) cast iron front cover; (c) polycarbonate front cover.

Variant 6 ( $D = 116$ ,  $d = 56$ ,  $h = 22$ ;  $h_1 = 28$ ) has less weight.

In this case, the deformations in variant 6 were 0.18 mm in the aluminum front cover, 0.06 mm in the cast iron front cover, and 0.97 mm in the polycarbonate front cover (Figure 21).

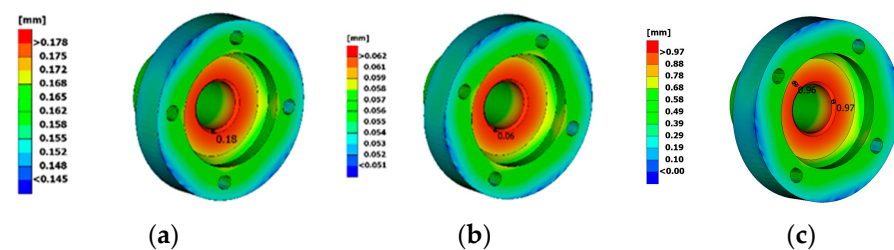


**Figure 21.** Deformations in the optimized design of the front cover of a gear pump: (a) aluminum front cover; (b) cast iron front cover; (c) polycarbonate front cover.

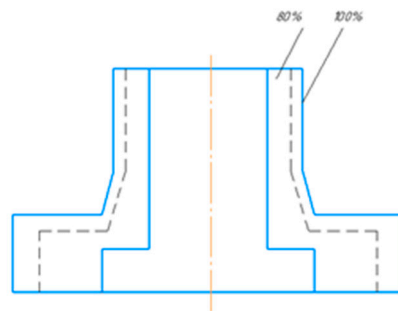
The design optimality criterion is based on Formula (7). The results of the optimization of the front pump cover by weight are presented in Table 10.



**Table 10.** The optimality criterion for the front pump cover.

Initial Mass, $m_0$ , kg	Final Mass, $m$ , kg	Safety Factor, $n$	Optimization Criteria, $F$
3.14	1.59	Aluminum	0.31
		Cast iron	
8.41	6.18	2.8	0.48
2.08	1.64	Polycarbonate (PC)	0.32
		3.1	

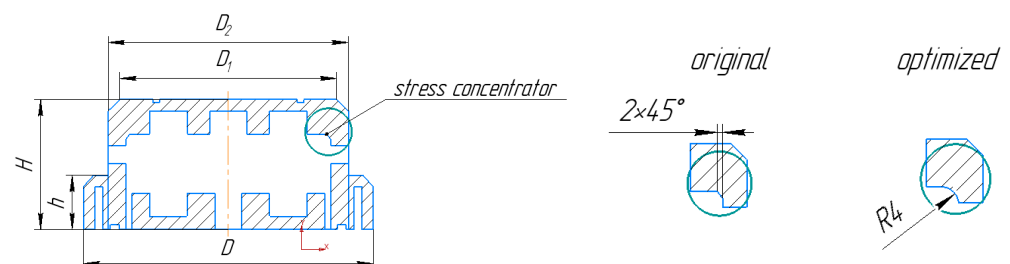
The polycarbonate front pump cover has less weight. However, according to the optimality criterion ( $F \rightarrow \min$ ), aluminum should be selected. The material consumption of the front cover was reduced by 20% (Figure 22).

**Figure 22.** Comparison of the size of the front cover before optimization (100%) and after optimization (80%).

Thus, the optimization of the front cover of a gear pump is permissible using aluminum because the optimality criterion is minimal.

#### 4.2.3. Optimization of the Gear Pump Casing

As the modeling has shown, the groove on the bottom of the casing, formed by a chamfer on the outside, is a stress concentrator. As this stress concentrator cannot be removed or moved, it is necessary to increase the cross-section of the groove by rounding it (Figure 23). Similar groove modifications have also brought about benefits in stress distribution in other studies [54,55].

**Figure 23.** Zone of maximum stress in the gear pump casing and a new technical solution.

The main parameters of the case are  $D = 186$  mm,  $h = 64$  mm,  $H = 118$  mm,  $D_1 = 166$  mm,  $D_2 = 158$  mm.

By replacing the  $2 \times 45^\circ$  chamfer with a rounding with radius  $R_4$ , a decrease in stress concentration was obtained in this zone.

The stress distribution pattern remains the same; however, at the bottom of the aluminum gear pump casing the stresses are  $(163 \div 167)$  MPa; at the bottom of the cast iron casing— $(140 \div 142)$  MPa; at the bottom of the polycarbonate casing— $(182 \div 189)$  MPa.

When comparing the results before and after optimization, it was found that in the aluminum casing the stresses decreased by 10 MPa; in the cast iron casing the stresses decreased by 12 MPa; and in the polycarbonate casing the stresses decreased by 11 MPa.

When parametrically optimizing the gear pump parts, the total weight of the aluminum pump was reduced by 2.19 kg. The weight of the cast iron pump was decreased by 3.63 kg. The weight of the polycarbonate casing decreased by 0.6 kg.

According to the obtained data, the polycarbonate gear pump has less weight. However, aluminum should be chosen because aluminum was selected for the front and back covers based on the optimality criterion. In addition, it is technologically easier to manufacture aluminum gear pump parts, particularly the internal surfaces of the casing, which have a complex profile. Currently, cast iron [56] and aluminum [57] are still popular materials for pump bodies, but intensive work is underway on the introduction of plastics [47].

## 5. Conclusions

The strength analysis of a gear pump casing design can indicate the areas where material reduction work can be performed. The study presents areas of the gear pump casing (mainly in 3D model graphics) that may be subject to weight reduction procedures according to the process and the operational processes. In the case of a newly developed gear pump, the areas most susceptible to stress concentration are the grooves in the lower part of the pump casing. For the rear cover, the stress concentrator is its central part and is described by the contour on which the flange is located. For the front cover, the most stressed area is the beginning of the outlet through which the pumped liquid exits.

With the same geometry, the stress in a cast iron body relative to an aluminum casing is 11% lower. The stress in a cast iron body is 34% lower compared to a carbonate casing. When assessing the strength of the gear pump casing, it was found that there are zones (the outer wall of the second stage of the pump casing, the central part of the cover under the drive shaft) with a maximum safety factor. Reinforcement of the hull structure is not required in these areas. There are also unloaded zones in the casing and back cover (case areas around the bearing slots, extreme zones in the back cover for bolts), where the safety factor values tend to infinity. Reducing the metal in these areas increases stress in the structure but does not affect the overall strength of the pump casing structure during operation.

Parametric optimization of the gear pump casing made it possible to reduce the weight of the aluminum structure by 14%, the weight of the cast iron structure by 12%, and the weight of the polycarbonate structure by 16% compared to the weight of the original design.

Focusing on the optimality criterion and the safety factor, it is necessary to choose aluminum for the manufacture of gear pump parts. From a technological point of view, this is also advisable.

Overall, this paper makes a valuable contribution to the field of gear pump design and optimization. The results presented in the article can be used to develop lighter and more efficient gear pumps.

The above-mentioned strength analysis with the criterion of weight minimization and material selection is applicable when designing new parts, structures, and equipment for the purpose of resource conservation.

This method can be used to generate new ideas for future advances in structure design and optimization while reducing material costs and time.

In the future, research will be carried out to find a comprehensive solution for the parametric and topological optimization of the aluminum gear pump casing to reduce weight and to reduce the overall cost of the gear pump. Further work is also needed to expand the validity of the proposed optimization procedure, including supplementing it with tools aimed at solving the problem of parts manufacturability.

This study has certain limitations related to the sensitivity to the initial guesswork, and there was no grid variation during the modeling. In future studies, we intend to address these shortcomings by improving the modeling algorithm.

**Author Contributions:** Conceptualization, Ł.G. and O.Z.; methodology, O.Z., Ł.G. and T.N.; software, A.B. (Andrey Berg); validation, Ł.G., O.Z. and D.Z.; formal analysis, O.Z. and T.N.; investigation, D.Z., A.B. (Alexandra Berg) and A.B. (Andrey Berg); resources, O.Z. and A.B. (Alexandra Berg); data curation, Ł.G. and Ł.W.; writing—original draft preparation, O.Z., Ł.G. and T.N.; writing—review and editing, O.Z., Ł.G., Ł.W., W.Ł. and K.F.; visualization, A.B. (Andrey Berg) and A.B. (Alexandra Berg); supervision, O.Z. and Ł.G.; project administration, T.N. and Ł.G. All authors have read and agreed to the published version of the manuscript.

**Funding:** This research is funded by the Science Committee of the Ministry of Science and Higher Education of the Republic of Kazakhstan (Grant of Young Scientists IRN No. AP19579208 “Creation of a universal prototype of a gear pump for hydraulic systems capable of pumping viscous liquids of various nature”). Analysis of the design and technological features of gear pumps.

**Institutional Review Board Statement:** Not applicable.

**Informed Consent Statement:** Not applicable.

**Data Availability Statement:** Data are contained within the article.

**Conflicts of Interest:** The authors declare no conflict of interest. The funders had no role in the design of the study; in the collection, analyses, or interpretation of data; in the writing of the manuscript; or in the decision to publish the results.

## References

1. Lakshmanana, K.; Tessicini, F.J.; Gil, A.; Auricchio, F. A fault prognosis strategy for an external gear pump using machine learning algorithms and synthetic data generation methods. *Appl. Math. Model.* **2023**, *123*, 348–372. [\[CrossRef\]](#)
2. Frosina, E.; Senatore, A.; Rigosi, M. Study of a High-Pressure External Gear Pump with a Computational Fluid Dynamic Modeling Approach. *Energies* **2017**, *10*, 1113. [\[CrossRef\]](#)
3. Muzzioli, G.; Montorsi, L.; Polito, A.; Lucchi, A.; Sassi, A.; Milani, M. About the Influence of Eco-Friendly Fluids on the Performance of an External Gear Pump. *Energies* **2021**, *14*, 799. [\[CrossRef\]](#)
4. Sherov, A.; Myrzakhetmet, B.; Sherov, K.; Absadykov, B.; Sikhimbayev, M. Method for selecting the location of the clearance fields of the landing surfaces of gear pump parts with a biaxial connection. *NEWS Acad. Sci. Repub. Kazakhstan* **2022**, *1*, 159–166. [\[CrossRef\]](#)
5. Ransegnola, T.; Zhao, X.; Vacca, A. A comparison of helical and spur external gear machines for fluid power applications: Design and optimization. *Mech. Mach. Theory* **2019**, *142*, 103604. [\[CrossRef\]](#)
6. Hao, X.; Zhou, X.; Liu, X.; Sang, X. Flow characteristics of external gear pumps considering trapped. *Adv. Mech. Eng.* **2016**, *8*, 1687814016674100. [\[CrossRef\]](#)
7. Keith, R. *Mobley Fluid Power Dynamics Chapter 3—Hydraulic Pumps*; Elsevier: Amsterdam, The Netherlands, 2000; pp. 25–46.
8. Richard, W. *Hanks Fluid Dynamics (Chemical Engineering) Encyclopedia of Physical Science and Technology*, 3rd ed.; Academic Press: Cambridge, MA, USA, 2003; pp. 45–70.
9. Hassan, A. Contact Stress Analysis of Spur Gear Teeth Pair. *Int. Sch. Sci. Res. Innov.* **2009**, *3*, 1279–1284.
10. Zhao, X.; Vacca, A. Theoretical Investigation into the Ripple Source of External Gear Pumps. *Energies* **2019**, *12*, 535. [\[CrossRef\]](#)
11. Egbe, E.A.P. Design Analysis and Testing of a Gear Pump Research Inventory. *Int. J. Eng. Sci.* **2013**, *3*, 1–7.
12. Osinski, P. *Modelling and Design of Gear Pumps with Modified Tooth Profile*; Lambert Press: Saarbrücken, Germany, 2014; 156p.
13. Rituraj, F.; Vacca, A. External gear pumps operating with non-Newtonian fluids: Modelling and experimental validation. *Mech. Syst. Signal Process.* **2018**, *106*, 284–302. [\[CrossRef\]](#)
14. Fadejkin, A.S.; Peshcherenko, M.P.; Gorbunov, A.V.; Peshcherenko, S.N. Gear Wheel Pump for Fluid Pumping. RU Patent 2,536,736, 27 December 2014.
15. Khramtsov, A.A.; Galperovich, L.G.; Klebanov, B.M.; Borisova, M.R.; Klyuev, O.N. Multi-Gear Pumps. USSR Patent 836387, 6 July 1981.
16. Zheng, Y. Gear Pump with Counterbalanced Radial Forces and Two Piece Radial Seals. USA Patent 5,161,961, 10 November 1992.
17. Patrushev, G.S.; Patrushev, S.G. Adjustable Reversible Gear Pump. RU Patent 2,194,190, 10 December 2002.
18. Li, P.; Zhao, Y.; Qing, C. Fracture Analysis of an Aluminum Alloy Gear Pump Casing. *Key Eng. Mater.* **2016**, *723*, 288–293. [\[CrossRef\]](#)
19. Vernon, E.E.; Stevenson, M.E.; McDougall, J.L. Lauren McCall Failure analysis of gray iron pump casings. *J. Fail. Anal. Prev.* **2004**, *4*, 15–18. [\[CrossRef\]](#)
20. Casoli, P.; Vacca, A.; Berta, G. Optimization of relevant design parameters of external gear pumps. *Proc. JFPS Int. Symp. Fluid Power* **2008**, *7*, 277–282. [\[CrossRef\]](#)
21. Wang, S.; Sakurai, H.; Kasarekar, A. The Optimal Design in External Gear Pumps and Motors. *IEEE/ASME Trans. Mechatron.* **2011**, *16*, 945–952. [\[CrossRef\]](#)
22. Ozsoya, M.; Kurnaz, C. An Optimization Study of a Hydraulic Gear Pump Cover with Finite Element Method. *Acta Phys. Pol. A* **2017**, *132*, 944–948. [\[CrossRef\]](#)

23. Houzeaux, G.; Codina, R. A Finite Element Method for the Solution of Rotary Pumps. *Comput. Fluids* **2007**, *36*, 667–679. [\[CrossRef\]](#)
24. Cieřlicki, R.; Karliński, J.; Osiński, P. Numerical Model of an External Gear Pump and Its Validation. In Proceedings of the 14th International Scientific Conference: Computer Aided Engineering, Wrocław, Poland, 20–23 June 2018; Springer: Berlin/Heidelberg, Germany, 2019; pp. 96–103.
25. Kattimani, K.D.; Tavildar, R.K.; Kakamari, P.P. Finite element analysis and optimization of external gear pump. *JETIR* **2016**, *3*, 119–126.
26. Xie, Q. Numerical modeling of the stress-strain state of the ice beam by specified constitutive model. *Mater. Sci. Eng. Appl.* **2022**, *2*, 1–8. [\[CrossRef\]](#)
27. Farahani, B.; Amaral, R.; Tavares, P.; Moreira, P.; Santos, A. Material characterization and damage assessment of an AA5352 aluminum alloy using digital image correlation. *J. Strain. Anal.* **2020**, *55*, 3–19. [\[CrossRef\]](#)
28. Li, H.; Yang, J.; Chen, G.; Liu, X.; Zhang, Z.; Li, G.; Liu, W. Towards intelligent design optimization: Progress and challenge of design optimization theories and technologies for plastic forming. *Chin. J. Aeronaut.* **2021**, *34*, 104–123. [\[CrossRef\]](#)
29. Nguyen, T.; Huynh, N.; Vu, N.; Kieu, V.; Huang, S. Optimizing compliant gripper mechanism design by employing an effective bi-algorithm: Fuzzy logic and ANFIS. *Microsyst. Technol.* **2021**, *27*, 3389–3412. [\[CrossRef\]](#)
30. Scheaua, F. Assembly design optimization for gear pump hydraulic units. *J. Ind. Des. Eng. Graph.* **2012**, *7*, 15–18.
31. Wang, C.N.; Yang, F.C.; Nguyen, V.T.T.; Vo, N.T. CFD analysis and optimum design for a centrifugal pump using an effectively artificial intelligent algorithm. *Micromachines* **2022**, *13*, 1208. [\[CrossRef\]](#)
32. Jeevanantham, A.; Pandivelan, C. Topology and shape optimization of gear casing using finite element and Taguchi based statistical analyses. *ARPJ. Eng. Appl. Sci.* **2016**, *11*, 13721–13733.
33. Zuo, Z.; Liu, S.; Fan, Y.; Wu, Y. Optimization of a centrifugal boiler circulating pump's casing based on CFD and FEM analyses. *Adv. Mech. Eng.* **2014**, *6*, 532892. [\[CrossRef\]](#)
34. Zhang, L.; Tang, L.; Wen, Q.; Luo, W. Study on optimization of pump shaft transmission system of plastic centrifugal pump. *J. Eng.* **2022**, *2022*, 4905247. [\[CrossRef\]](#)
35. Qin, Y.; Qi, Q.; Shi, P.; Scott, P.; Jiang, X. Status, issues, and future of computer-aided part orientation for additive manufacturing. *Int. J. Adv. Manuf. Technol.* **2021**, *115*, 1295–1328. [\[CrossRef\]](#)
36. Antoniou, A.; Lu, W.-S. *Practical Optimization. Algorithms and Engineering Applications*; Springer: Berlin/Heidelberg, Germany, 2007; 669p.
37. Mamat, M.; Dauda, M.K.; Mohamed, M.A.; Waziri, M.Y.; Mohamad, F.S.; Abdullah, H. Derivative free Davidon-Fletcher-Powell (DFP) for solving symmetric systems of nonlinear equations. *IOP Conf. Ser. Mater. Sci. Eng.* **2018**, *332*, 012030. [\[CrossRef\]](#)
38. Wilson, P. *Chapter 16—Design Optimization Design Recipes for FPGAs*, 2nd ed.; Elsevier: Amsterdam, The Netherlands, 2016; pp. 231–235.
39. Norman, E. *Dowling Mechanical Behavior of Materials: Engineering Methods for Deformation, Fracture, and Fatigue*, 4th ed.; Pearson Education Limited: Upper Saddle River, NJ, USA, 2013; 920p.
40. Mobarakeh, M.; Farhatnia, F. Thermo Elasto-Plastic analysis of functionally graded thick-walled cylindrical shells based on Prandtl-Reuss flow rule. *Modares Mech. Eng.* **1999**, *99*, 211–218. (In Persian)
41. Kutz, M. *Mechanical Engineers' Handbook, Materials and Engineering Mechanics*; John Wiley & Sons, Inc.: Hoboken, NJ, USA, 2015; 1043p.
42. Rennert, R.; Kulling, E. *Rechnerischer Festigkeitsnachweis für Maschinenbauteile aus Stahl, Eisenguss- und Aluminiumwerkstoffen*; Forschungskuratorium Maschinbau (FKM): Frankfurt, Germany, 2020; 230p.
43. Draper, N.; Smith, G. *Applied Regression Analysis. Finance and Statistics*; John Wiley & Sons: Hoboken, NJ, USA, 1986; 366p.
44. Rawlings, J.; Pantula, S.; Dickey, D. *Applied Regression Analysis a Research Tool Textbook Springer Texts in Statistics (STS)*; Springer: Berlin/Heidelberg, Germany, 1998; 456p.
45. Zhang, Z.; Zhao, W.; Sun, Q.; Li, C. Theoretical Calculation of the Strain-Hardening Exponent and the Strength Coefficient of Metallic Materials. *J. Mater. Eng. Perform.* **2006**, *15*, 19–22. [\[CrossRef\]](#)
46. Jorga, C.; Desrochers, A.; Smeesters, C. Engineering Design from a Safety Perspective. In Proceedings of the 2012 Canadian Engineering Education Association (CEEAA12), Winnipeg, MB, Canada, 17–20 June 2012; pp. 1–5.
47. Mancini, S.D.; Santos Neto, A.D.O.; Cioffi, M.O.H.; Bianchi, E.C. Replacement of metallic parts for polymer composite materials in motorcycle oil pumps. *J. Reinf. Plast. Compos.* **2017**, *36*, 149–160. [\[CrossRef\]](#)
48. Kollek, W.; Radziwanowska, U. Energetic efficiency of gear micropumps. *Arch. Civ. Mech. Eng.* **2015**, *15*, 109–115. [\[CrossRef\]](#)
49. Mali, P.S.; Joshi, G.S.; Patil, I.A. CFD Simulation of External Gear Pump using ANSYS CFX. *Int. J. Appl. Eng. Res.* **2018**, *13*, 11970–11973.
50. Kollek, W.; Osiński, P.; Warzyńska, U. The influence of gear micropump body asymmetry on stress distribution. *Pol. Marit. Res.* **2017**, *24*, 60–65. [\[CrossRef\]](#)
51. Qi, F.; Dhar, S.; Nichani, V.H.; Srinivasan, C.; Wang, D.M.; Yang, L.; Bing, Z.; Yang, J.J. A CFD study of an electronic hydraulic power steering helical external gear pump: Model development, validation and application. *SAE Int. J. Passeng. Cars Mech. Syst.* **2016**, *9*, 346–352. [\[CrossRef\]](#)
52. Cinar, R.; Ucar, M.; Celik, H.K.; Firat, M.Z.; Rennie, A.E.W. Pressure determination approach in specific pressure regions and FEM-based stress analysis of the housing of an external gear pump. *Exp. Tech.* **2016**, *40*, 489–499. [\[CrossRef\]](#)

53. De Martin, A.; Jacazio, G.; Sorli, M. Optimization of gerotor pumps with asymmetric profiles through an evolutionary strategy algorithm. *Machines* **2019**, *7*, 17. [\[CrossRef\]](#)
54. Zeng, D.; Zhang, Y.; Lu, L.; Zou, L.; Zhu, S. Fretting wear and fatigue in press-fitted railway axle: A simulation study of the influence of stress relief groove. *Int. J. Fatigue* **2019**, *118*, 225–236. [\[CrossRef\]](#)
55. Liu, G.; Huang, C.; Su, R.; Özel, T.; Liu, Y.; Xu, L. 3D FEM simulation of the turning process of stainless steel 17-4PH with differently texturized cutting tools. *Int. J. Mech. Sci.* **2019**, *155*, 417–429. [\[CrossRef\]](#)
56. Alzafin, Y.A.; Mourad, A.H.; Abou Zour, M.; Abuzeid, O.A. Stress corrosion cracking of Ni-resist ductile iron used in manufacturing brine circulating pumps of desalination plants. *Eng. Fail. Anal.* **2009**, *16*, 733–739. [\[CrossRef\]](#)
57. Battarra, M.; Mucchi, E. Incipient cavitation detection in external gear pumps by means of vibro-acoustic measurements. *Measurement* **2018**, *129*, 51–61. [\[CrossRef\]](#)

**Disclaimer/Publisher's Note:** The statements, opinions and data contained in all publications are solely those of the individual author(s) and contributor(s) and not of MDPI and/or the editor(s). MDPI and/or the editor(s) disclaim responsibility for any injury to people or property resulting from any ideas, methods, instructions or products referred to in the content.